Period-two cycles in a feedforward layered neural network model with symmetric sequence processing

F. L. Metz and W. K. Theumann
Instituto de Física, Universidade Federal do Rio Grande do Sul, Caixa Postal 15051, 91501-970 Porto Alegre, Brazil
(Received 8 May 2006; revised manuscript received 10 November 2006; published 12 April 2007)

The effects of dominant sequential interactions are investigated in an exactly solvable feedforward layered neural network model of binary units and patterns near saturation in which the interaction consists of a Hebbian part and a symmetric sequential term. Phase diagrams of stationary states are obtained and a phase of cyclic correlated states of period two is found for a weak Hebbian term, independently of the number of condensed patterns c.

DOI: 10.1103/PhysRevE.75.041907 PACS number(s): 87.10.+e, 64.60.Cn, 07.05.Mh

I. INTRODUCTION

The dynamics and the stationary states of recurrent attractor neural networks that process sequences of patterns have been studied over some time and there has been a recent revival of interest near the storage saturation limit in large networks [1–8]. Either a process involving a sequence of patterns [3–7] (referred to in this paper as asymmetric sequence processing), leading to a stationary limit cycle, or a process involving a pair of sequences, one with patterns in increasing order and the other one with patterns in decreasing order (referred to as symmetric sequence processing in what follows), was considered in those works.

Symmetric sequence processing competing with pattern reconstruction favored by a Hebbian term of fixed strength has also been considered [1,8]. The ratio J_H/J_S between the strengths J_H and J_S of the Hebbian term and of the pair of sequences, respectively, has been restricted to a mostly dominant Hebbian strength, that is, to $1 \leqslant J_H/J_S \leqslant \infty$, leading to phase diagrams that exhibit only fixed-point solutions including nontrivial correlated attractors [1,8]. These are states that indicate a selectivity in response to a set of previously learned patterns in which the correlation coefficients for the attractors with increasingly distant patterns from a stimulus are decreasing functions which eventually become vanishingly small. The sequential part of the interaction induces transitions between patterns, whereas a sufficiently strong Hebbian term locks the transitions, favoring single-pattern recognition. The case of network models with a weak Hebbian interaction competing with a dominating symmetric sequential processing in which $J_H/J_S < 1$ has, apparently, not been studied before and it is important to find out what kind of solutions appear in that case and their possible biological implications.

Indeed, the connection between the information input in a network of contiguous stimuli in a training sequence of uncorrelated patterns and correlated delay activity as an output has been of great interest to explain the results of experimental recordings of a visual-memory task in the inferotemporal (IT) cortex of monkeys [8–13], in which correlated states play an essential role. The results can be interpreted as a connection between persistent cortex activity and long-term associative memory described by a fixed-point attractor dynamics, and the early model calculations that have been done are based on the competition between pattern reconstruction and symmetric sequence processing [1,11].

There could be other attractors that may predict further behavior on visual memory in the primate IT cortex viewed as a dynamical system, generating either limit cycles or chaotic or other kinds of behavior. Earlier model calculations on the competition between pattern reconstruction and asymmetric sequence processing exhibit periodic and stationary fixed-point attractors, besides quasistationary states [14,15]. Motivated by the results that appeared in the type of experiments on the IT cortex in monkeys and their interpretation [1,8–13], it would be interesting to see if there are periodic attractors that appear as correlated states in a neural network model with the kind of competition between pattern reconstruction and symmetric sequence processing that has been studied before in a recurrent network [1,11], now with a weak Hebbian term. The presence of periodic attractors would suggest a new kind of persistent oscillating activity in the IT cortex. The main purpose of this work is to explore this issue and with that in mind one has to resort to a dynamical procedure even to detect stationary cyclic behavior and to determine the emergent properties.

Since the dynamics of fully recurrent neural networks with binary units is already fairly complicated, and even more so with graded response or other more realistic units, we make a drastic simplification to start with in order to get to the essentials of our issue. We are mainly interested in finding out if there are cyclic attractors and in characterizing their properties for a sizable critical storage of patterns. Our interest is in the role of competing interactions that favor either transitions between patterns or the recognition of specific patterns. To that end we focus on a simple attractor feedforward layered network model of binary units and patterns with a parallel dynamics and without lateral connections [16]. The model is exactly solvable and has been extensively used in the past as a model for associative memory that has all the stationary features of a recurrent network and it is particularly suited to detect stationary nonequilibrium states. We show that, despite sequential learning, the procedure involves in practice a finite number of recursion relations even for a macroscopically large system. The effect of the lateral connections is to change the quantitative results of the model.

To make that point clear we construct the phase diagrams that describe the network behavior for an arbitrary strength

of the Hebbian term in order to check first that we get the same qualitative behavior as that already found for a recurrent network in the case of balanced interactions or for a dominant Hebbian term. Having studied that part, one can be reasonably confident that the behavior of the layered network for dominant sequential interaction should also describe the correct qualitative behavior of a recurrent network. The fully quantitative behavior of that network is a relevant issue which is beyond the scope of the present paper.

It will be shown that a phase of cyclic stationary solutions of period two is obtained, independently of the number of condensed patterns c with macroscopic overlap with the states of the network, and that this is a phase of nontrivial correlated states. These are states that could reflect a new kind of persistent activity in visual-memory task experiments. On the other hand, the stability of the cyclic phase is strongly dependent on c. These features distinguish the properties of the present model from those for asymmetric sequence processing competing with pattern reconstruction where cycles of period c appear, for arbitrary c [15].

The purpose of studying a simplified model which has the qualitative features of a recurrent network with more realistic interactions is that it tells what to look for and what could be relevant in a more biological type of network. The paper is organized as follows. In Sec. II we present the model and outline the derivation of the dynamics with the aid of an Appendix. We present our main results in Sec. III and conclude with a further discussion in Sec. IV.

II. THE MODEL AND THE DYNAMICS

The network model consists of L layers, each containing N binary units (neurons) in states $S_i(l)=\pm 1$, where i denotes the unit and l the layer. The state $+1$ represents a firing unit and the state -1 a unit at rest. The state of each unit on a given layer is determined in parallel by the state of all units on the previous layer, the layer label acting as a time step, according to the stochastic rule with probability [16]

$$P(S_i(l+1)|\boldsymbol{S}(l)) = \frac{\exp[\beta S_i(l+1)h_i(l+1)]}{2\cosh[\beta h_i(l+1)]}, \tag{1}$$

$$h_i(l+1) = \sum_{j=1}^{N} J_{ij}(l)S_j(l), \tag{2}$$

where $h_i(l+1)$ is the local field at unit i on layer $l+1$ due to the set of states $\boldsymbol{S}(l)$ of all units on layer l and $J_{ij}(l)$ is the synaptic coupling between unit j on layer l and unit i on layer $l+1$. There is no feedback in the updating of the units and the first layer has to be set externally in a given state. The parameter $\beta=T^{-1}$ controls the synaptic noise such that the dynamics is fully deterministic when $T\to 0$ and fully random when $T\to\infty$.

A macroscopic set of $p=\alpha N$ statistically independent and identically distributed random patterns $\{\boldsymbol{\xi}^{\mu}(l)\}$, $\mu=1,\ldots,p$, with components $\xi_i^{\mu}(l)=\pm 1$ and probability $\frac{1}{2}$ for either value, are stored on every layer independently of other layers, according to the learning rule

$$J_{ij}(l) = \frac{1}{N}\sum_{\mu,\rho=1}^{p} \xi_i^{\mu}(l+1)X_{\mu\rho}\xi_j^{\rho}(l). \tag{3}$$

Thus, there are only interactions between pairs of units on consecutive layers. Connections between units on more distant layers, as well as lateral connections between units on the same layer, are excluded. Here, $X_{\mu\rho}$ are the elements of the matrix

$$\boldsymbol{X} = \begin{pmatrix} \boldsymbol{A} & 0 \\ 0 & \boldsymbol{B} \end{pmatrix},$$

and

$$A_{\mu\rho} = \nu\delta_{\mu,\rho} + (1-\nu)(\delta_{\mu,\rho+1} + \delta_{\mu,\rho-1}),$$

$$B_{\mu\rho} = b\,\delta_{\mu,\rho} + (1-b)(\delta_{\mu,\rho+1} + \delta_{\mu,\rho-1}) \tag{4}$$

are the elements of the $c\times c$ and $(p-c)\times(p-c)$ blocks $\boldsymbol{A}$ and $\boldsymbol{B}$ responsible for the signal and for the noise in the local field, respectively, and c is the number of condensed patterns that yield macroscopic overlaps defined below. The diagonal two-block interaction matrix reflects the fact that the patterns are associated in two independent cycles, one for the condensed patterns $[\boldsymbol{\xi}^{c+1}(l)=\boldsymbol{\xi}^{1}(l)]$ and the other one for the noncondensed patterns $[\boldsymbol{\xi}^{p+1}(l)=\boldsymbol{\xi}^{c+1}(l)]$. This guarantees the applicability of the procedure. The first parts of $\boldsymbol{A}$ and $\boldsymbol{B}$ contribute to a Hebbian interaction J_H and their second parts contribute to the symmetric sequential interaction J_S. The training of the network model may be thought to proceed in two stages assuming the patterns are numbered in a given order. In one stage the set of patterns is presented to the network in random order, every pattern being presented the same number of times. This builds up the Hebbian part of the learning rule, whereas the sequential part of the rule takes place as follows in another stage. The patterns are ordered in two sequences, one sequence in increasing order in which each pattern is presented with the following pattern in the sequence, and the other sequence in decreasing order where every pattern is presented with the previous pattern.

The crucial parameter is ν, determining the ratio J_H/J_S of the Hebbian to sequential interaction in the signal term of the local field. On the other hand, different sequential noise levels given by b should yield qualitatively similar results as found in previous works [1,15]. This does not mean that b is an irrelevant parameter and we consider this point below. When $b=1$ there is a purely Hebbian noise and for any other b there is a Hebbian plus sequential noise. In distinction to other works, the choice $(0\leqslant\nu,b\leqslant 1)$ enables us to explore the full range of parameters ν and b.

The macroscopic overlap components $m_{\mu}(l)$ of $O(1)$, between the configuration $\boldsymbol{S}(l)$ and the condensed patterns, are given by the large-N limit of

$$m_N^{\mu}(l) = \frac{1}{N}\sum_{i=1}^{N} \xi_i^{\mu}(l)\langle S_i(l)\rangle, \quad \mu=1,\ldots,c, \tag{5}$$

where $\langle\cdots\rangle$ denotes a thermal average with Eq. (1), whereas the overlaps with the remaining $(p-c)$ noncondensed patterns are $M_N^{\mu}(l)=O(1/\sqrt{N})$.

Following the standard procedure for the layered network, one may write the local field as a sum of a signal and a noise term $\omega_i(l)$ due to the condensed and the noncondensed patterns, respectively [16]. The noise follows a Gaussian distribution with mean zero and a variance $\Delta^2(l)$ given by the large-N limit of

$$\Delta_N^2(l) = \sum_{\mu=c+1}^{p} \overline{\langle Q_N^\mu(l)^2 \rangle}, \tag{6}$$

where the overbar denotes the average over all the patterns, in which

$$Q_N^\mu(l) = bM_N^\mu(l) + (1-b)[M_N^{\mu-1}(l) + M_N^{\mu+1}(l)]. \tag{7}$$

The noncondensed overlaps that appear here depend on all patterns as functions of the full local field. Averages over the noncondensed patterns can then be performed by integration and we obtain first the recursion relations for the macroscopic overlaps $\boldsymbol{m}(l)=(m_1(l),\ldots,m_c(l))$,

$$\boldsymbol{m}(l+1) = \left\langle \boldsymbol{\xi} \int Dz \tanh\{\beta[\boldsymbol{\xi}\cdot \boldsymbol{A}\boldsymbol{m}(l) + \Delta(l)z]\} \right\rangle_{\boldsymbol{\xi}}, \tag{8}$$

where $Dz=e^{-z^2/2}dz/\sqrt{2\pi}$ and $\langle\cdots\rangle_{\boldsymbol{\xi}}$ denotes an explicit average over the condensed patterns which does not depend on the specific realization of the patterns.

To obtain a dynamic equation for $\Delta^2(l)$ we need recursion relations not only for the average squared noncondensed overlaps $\overline{\langle M_N^\mu(l)^2\rangle}$ and $\overline{\langle M_N^{\mu\pm1}(l)^2\rangle}$, which can be derived in the usual way [16], but also for the correlation of two consecutive overlaps and two next-to-consecutive overlaps, $\overline{\langle M_N^\mu(l)M_N^{\mu\pm1}(l)\rangle}$ and $\overline{\langle M_N^{\mu-1}(l)M_N^{\mu+1}(l)\rangle}$, respectively. These generate, in turn, correlations of overlaps between more distant patterns, which requires us to keep track of the general form [15]

$$C_n^2(l) = \sum_{\mu=c+1}^{p} \overline{\langle Q_N^\mu(l)Q_N^{\mu+n}(l)\rangle}, \tag{9}$$

in which $n=0,\ldots,p-c-1$ and $C_{p-c}(l)=\Delta(l)$. The $p-c$ recursion relations for the C_n's can be obtained in a systematic way, as outlined in the Appendix, leading to a variance of the noise which depends on the spin-glass order parameter $q(l)=\overline{\langle S(l)\rangle^2}$,

$$q(l) = \left\langle \int Dz \tanh^2\{\beta[\boldsymbol{\xi}\cdot \boldsymbol{A}\boldsymbol{m}(l) + \Delta(l)z]\} \right\rangle_{\boldsymbol{\xi}}. \tag{10}$$

In the case where $b=1$ (Hebbian noise), the variance follows the simple form $\Delta^2(l+1)=\alpha+K^2(l)\Delta^2(l)$, where $K(l)=\beta(1-q(l))$. In the case of the absence of stochastic noise ($\alpha=0$), the equations coincide with those for a recurrent network with a parallel dynamics. The main difference between the layered and the recurrent networks is the absence of recurrent connections in the former. The recurrent connections tend to amplify the effects produced by the stochastic noise and the fact that the equations are the same when $\alpha=0$ is simply due to the absence of noise to amplify in the recurrent network in that case. In the absence of stochastic noise the equations are also the same for the recurrent network with either symmetric or asymmetric extreme dilution [2].

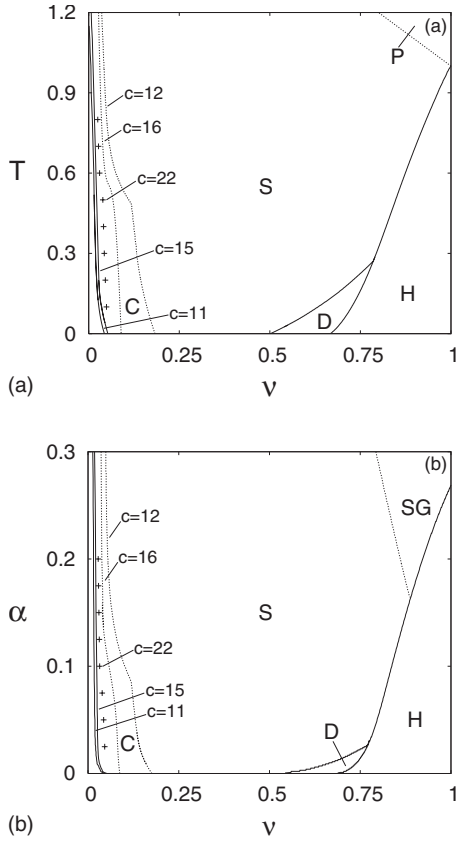

FIG. 1. Phase diagrams for (a) $\alpha=0$ and (b) $T=0$ with a purely Hebbian noise ($b=1$). The dotted and full lines indicate, respectively, continuous and discontinuous transitions and the phases are described in the text. Some points on the phase boundary for $c=22$ are indicated with crosses.

Thus, the network dynamics is described by the recurrence relations for the vector overlap (8) and for all the C_n's that go into the variance of the noise. Although the equations form an infinite set in the $p\to\infty$ limit, the number of significant C_n's is finite, making the model solvable in practice. The transients and the dynamic evolution of the network can be studied in full detail but here we restrict ourselves to the stationary states.

III. RESULTS

Consider first the (T,ν) phase diagram of stationary states for $\alpha=0$ and various numbers of condensed patterns c, shown in Fig. 1(a). The Hopfield ansatz $m_\mu(1)=\delta_{\mu,1}$, for $\mu=1,\ldots,c$, is used as initial condition. The states corresponding to fixed-point solutions and the phase boundaries for $\nu>0.5$ are precisely the same as those found for a recurrent network [1], since the equations for the order parameters are exactly the same in the layered and in the recurrent networks when $\alpha=0$. The Hopfield-like states (H) have one large condensed overlap component and the others are either small or zero. The phase of symmetriclike states (S) has equal or nearly equal overlap components, at high or low T, respec-

tively, ending at a paramagnetic phase (P), with $\boldsymbol{m}=\mathbf{0}$ and $q=0$. There is also a phase of nontrivially correlated states (D) in which the correlation coefficients for the overlaps with increasingly distant patterns from a stimulus become gradually smaller, as will be seen below. The phase boundaries for $\nu>0.5$ are practically independent of c.

The unusual features of the phase diagrams are stationary cyclic solutions (C) of period two, for any c, in the region $0<\nu\lesssim 0.5$ in which $\boldsymbol{m}(l+2)=\boldsymbol{m}(l)$. These are the only stable states below the phase boundaries for the presence of cyclic states. The main difference from the asymmetric sequence processing studied in an earlier work [15] is the presence in that case of cycles of period c, as well as quasiperiodic states. Figure 1 now shows that the size of the cyclic phase decreases or increases with an increase of c, if c is even or odd, respectively, and there are no cyclic solutions for $c<7$ in the latter case. These properties have been checked by a linear stability analysis of the S phase for $\alpha=0$ in extension of earlier work [14]. Clearly, the periodic solutions are fairly robust to synaptic noise T. In relation to a recent work [7], we also studied our model with a finite number of independent pairs of sequences for $\alpha=0$ and low ν and found only cyclic solutions of period two, for any number of stored sequence pairs and for any c in each sequence.

The effects of stochastic noise due to a macroscopic number of patterns $p=\alpha N$ are shown in Fig. 1(b) for $T=0$, $b=1$ (Hebbian noise) and various c. For the noncondensed overlaps we choose the initial $C_n^2(1)=\alpha$, for all n, and for the condensed overlaps we take again a Hopfield initial condition. As usual in the layered network, there is now a spin-glass phase with $q\neq 0$ (labeled SG). For $\nu=1$ we recover the critical storage ratio $\alpha_c\simeq 0.269$ for the Hebbian layered network model [16]. Also here we find the same kind of stationary states as in Fig. 1(a) for $\nu>0.5$ and stationary cyclic states of period two in the region of low ν, with the absence of the latter for $c<7$ in the case of odd c. Again, the boundaries between phases of fixed-point states are fairly independent of c, while the cyclic phase boundaries have a similar dependence on c as in the (T,ν) phase diagram. We also found that the cyclic phase boundaries almost do not vary beyond $c=11$ and $c=22$, for odd and even c, respectively. They are very close and they should be independent of c in the large-c limit.

Although Fig. 1 gives a fair account of the phase diagram for Hebbian noise ($b=1$), one may ask which is the effect of other noise parameters ($b\neq 1$) and in Fig. 2 we show the critical values α_c for the existence of two typical states in each of the phases H and C as functions of b, for $c=13$ and $T=0$. In the case of fixed-point states, that is, within the phase H (and also for the D phase, not shown in the figure), α_c increases with increasing ν for a given b, whereas in the case of cyclic states α_c decreases, as one would expect. Similar results are obtained for $c=12$. There is a maximum α_c for an optimal $b\simeq 0.748$ and the kind of noise becomes more relevant for a dominant sequential part (small ν) in the signal of the local field.

We consider next the solutions for the stationary overlaps that describe the long-time behavior of the network, for a weak Hebbian term. The overlaps for states in the phase

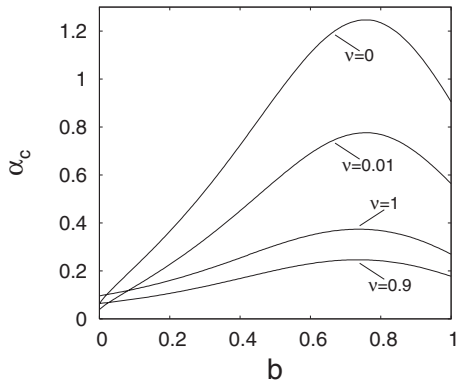

FIG. 2. Critical storage ratio as a function of b for $T=0$ and $c=13$ in the Hopfield-like phase ($\nu=1$ and 0.9) and in the cyclic phase ($\nu=0$ and 0.01).

diagrams bifurcate from a fixed-point behavior in the S phase to stable stationary limit cycles on the continuous (discontinuous) transition from the S to the C phase, for even (odd) c, respectively. In order to describe one of our main results, that is, the nature of the cyclic behavior, we illustrate this for the overlaps in Fig. 3 for $c=13$ when $\alpha=0$ for a typical low synaptic noise of $T=0.3$. The bifurcation diagram contains the stationary values of the first seven overlaps as functions of ν, with $m_\mu(1)=\delta_{\mu,1}$ as an initial condition. Each overlap assumes a larger and a smaller value in the cyclic phase marked with the same symbols (for clarity, only the larger one is labeled), with a decreasing oscillation amplitude as we move away from the stimulated pattern. For considerably higher noise levels, say $T=1.25$ and appropriate values of ν (see below), all the pairs of overlap components keep oscillating between the same upper and lower values. Thus, for such high levels of T, the cyclic phase is already a phase of a pair of symmetric states, one with all equal larger condensed overlaps and the other with all equal smaller overlaps. In addition, the overlap components have the symmetry $m_{\mu+n}(t)=m_{\mu-n}(t)$, where μ is the stimulated pattern and $n=1,\ldots,(c-1)/2$.

In the case of even c, there is first a continuous transition to a pair of overlaps with decreasing ν such that all solutions keep oscillating between an upper and a lower value. There

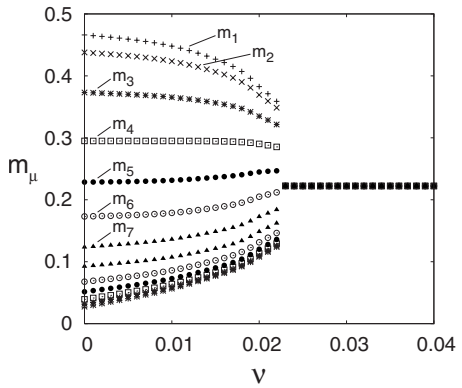

FIG. 3. Overlaps for the stationary cycles of period two, discussed in the text, that bifurcate from the symmetric phase for $c=13$, $\alpha=0$, and $T=0.3$.

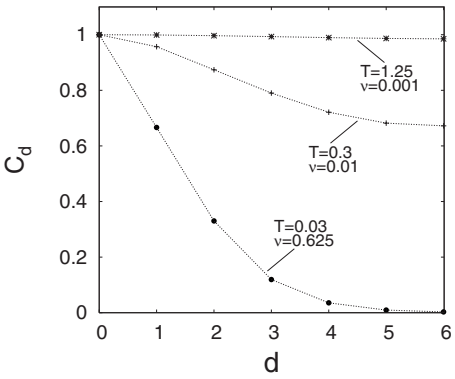

FIG. 4. Correlation coefficients between attractors as a function of the distance d from a reference pattern, defined in the text, for $c=13$ and $\alpha=0$ in the phases C (two upper curves) and D (lower curve). The lines are a guide to the eye.

is a further, discontinuous transition, for lower values of ν, to distinct pairs of overlaps that is similar to the discontinuous transition for the case of odd c, with the same symmetry between overlaps now for $n=1,\ldots,(c-2)/2$. Thus, the behavior of the overlap components has a rich structure which depends on whether c is even or odd.

In order to demonstrate that the cyclic states may be nontrivial correlated attractors for low ν, we consider next the correlation coefficients between the attractors corresponding to any two condensed patterns, ξ^μ and ξ^ν a distance $d=|\mu-\nu|$ away, defined here as

$$C_d = \frac{1}{C}\sum_i (\langle\sigma_i^\mu\rangle - \overline{\langle\sigma_i^\mu\rangle})(\langle\sigma_i^\nu\rangle - \overline{\langle\sigma_i^\nu\rangle})$$

$$= \frac{\langle\tanh(\beta h^\mu)\tanh(\beta h^\nu)\rangle_\xi}{\langle\tanh^2(\beta h^\mu)\rangle_\xi}, \qquad (11)$$

where $\langle\sigma_i^\rho\rangle$ is the attractor corresponding to the initially stimulated pattern ρ and $\overline{\langle\sigma_i^\rho\rangle}$ is its mean value over the network which is zero for the unbiased patterns we are using here.

We show in Fig. 4 the dependence of the correlation coefficients for the states corresponding to the larger overlap component of each pair of states with the distance d to increasingly distant condensed patterns in the sequence from a given stimulated one, for $c=13$ and $\alpha=0$, that is, in the absence of stochastic noise where the results are the same for the layered and the recurrent network. We do this, as indicated, for $(T,\nu)=(0.3,0.01)$ and also for (1.25, 0.001) both within the phase of cyclic states. In the first case, where each overlap component assumes distinct larger and smaller values, there are also correlation coefficients for the smaller values, not shown in the figure, which turn out to decrease less rapidly than the coefficients for the larger values. The reason for this is that there is a weaker distinction between the smaller components than among the larger ones. For the higher $T=1.25$ the correlation coefficients are already independent of d due to the fact that all the pairs of overlap components are oscillating between the same upper and lower values.

In distinction to the fixed-point correlated states in phase D, shown for our model by the lower set of results in the figure for $T=0.03$ and $\nu=0.625$, the correlation coefficients for the cyclic states do not decrease to zero and, instead, exhibit a behavior typical of quasisymmetric states for low T.

IV. DISCUSSION

To summarize our results, we obtained a closed-form attractor dynamics for a feedforward layered network model of binary units and patterns in terms of a finite number of macroscopic order parameters for the competition between pattern reconstruction and symmetric sequence processing. The dynamics is a parallel one, in which all units in each layer are updated simultaneously, and the work presented here is restricted to the stationary states of the dynamics which exhibits either fixed-point or cyclic behavior of period two, depending on the relative strength of the interactions. Either kind of behavior is an emergent property of the network which is an outcome of the dynamics.

Full phase diagrams of stationary network behavior were obtained, either for a finite loading of patterns or in the saturation limit for the storage of a macroscopic number of patterns. In the case of a balanced or dominant Hebbian term, that is, for $\nu \geqslant 0.5$, we obtained qualitatively the same phase diagrams as those found in work by previous authors for a recurrent attractor network exhibiting Hopfield-like states, correlated states, and symmetric ordered states [1]. This suggests that the layered network dynamics discussed here may also serve to make qualitative predictions about a recurrent network in the case of a weak Hebbian term. Of course, to get the right quantitative behavior expected for a recurrent network in the storage saturation limit, and for detailed comparison with experiments, one has to start by including lateral connections between units in a layer but this involves a more complicated dynamics which is beyond the scope of this paper. For ν below 0.5 we have first a regime of symmetric fixed-point behavior and for smaller values of ν we find the cyclic attractors discussed in this work. These are states that have decreasing correlation coefficients with increasingly distant attractors from an initially stimulated pattern for a sizable range of synaptic noise.

The stationary overlaps between the states of the network and the condensed patterns describe the long-time behavior of the system. As we saw, the overlaps for states within the cyclic phase are always periodic with period two, oscillating either between a distinct pair of upper and lower values for each overlap component or between the same pair of values for all components, depending on the parity of c and on the state in the (α,T,ν) phase diagram. We argue that the cyclic behavior of period two is a property that follows essentially from the nature of the interactions, that is, from the strong symmetric sequential term, rather than being an artifact of the model due to the lack of lateral connections between the units or having binary units. First, in support of our claim, work in progress on the parallel dynamics of a fully connected recurrent network of binary units and patterns indicates, indeed, that there are exclusively cyclic states of period two in a finite region of the phase diagram [17]. Second,

we checked explicitly that numerical simulations with threshold-linear units [12] in our feedforward layered network yield only cyclic states of period two for typical low values of α and ν, at $T=0$. The specific regions of the phase diagram where distinct pairs of upper and lower values or the same pair of values for the overlaps appear depends, of course, on the details of the model.

The phase diagrams found in this work are quite different from those for *asymmetric* sequence processing [14,15]. Indeed, the latter exhibit a $\nu \Leftrightarrow (1-\nu)$ duality that appears in the form of symmetric phase diagrams with a correspondence between fixed-point solutions for large ν and stationary cycles of period c for small ν. There is, apparently, no such duality in the case of symmetric sequence processing and whenever stable cycles appear they are of period two, independently of the number of condensed patterns c. Also, the strong c dependence of the stability of the cyclic phase is in contrast with the results for asymmetric sequence processing, in which the boundary of the cyclic phase in practice does not depend on the number of condensed patterns [14,15].

Although the work presented here is restricted to a layered feedforward network with no lateral interactions, it is expected to exhibit further features of a recurrent network beyond those pointed out above, in particular, the robustness to both synaptic (T) and to stochastic noise (α) due to the noncondensed patterns over a sizable ratio $\nu/(1-\nu)$ of the relative strength of the Hebbian to sequential interaction [Figs. 1(a) and 1(b), respectively]. The robustness becomes stronger in the case of decreasing even values of the number of condensed patterns c and weaker for odd values of decreasing c.

The model used here has several limitations with respect to a closer to biological network which do not allow us to make the proper quantitative predictions to compare with experiments, mainly the binary full activity units, in place of continuous or integrate-and-fire neurons, and unbiased (high-activity) patterns, without lateral interactions between units in the same layer. Despite those limitations, there is the possibility of making extended qualitative predictions for the kind of visual-task experiments in the IT primate cortex and their interpretation in terms of correlated states in simple models for a recurrent network [8–12]. Those works provided a connection between a fixed-point attractor dynamics in a recurrent network and persistent activity in a biological system. Our work suggests a connection between a periodic attractor dynamics in a recurrent network trained with patterns in a random order and with patterns in a sequence and a kind of oscillating persistent activity in the IT cortex with the specific cyclic behavior discussed in this work. The original experiments were based on intensive training with patterns in a random order and with patterns in a sequence. One may argue that, if the training of a primate with visual patterns in random order, which is supposed to be a realization of a Hebbian rule, is not sufficiently strong, one may have a situation such as that described here for small ν with the presence of correlated cyclic states of period two, in which the correlation coefficients decay with increasing distance from the stimulus, up to a finite value.

The results presented here should stimulate further theoretical and experimental work for the case of weak Hebbian reenforcement of patterns. It may also lead to interesting applications in information processing in networks [18].

ACKNOWLEDGMENTS

The work of one of the authors (W.K.T.) was financially supported, in part, by CNPq (Conselho Nacional de Desenvolvimento Científico e Tecnológico), Brazil. Grants from CNPq and FAPERGS (Fundação de Amparo à Pesquisa do Estado de Rio Grande do Sul), Brazil, to the same author are gratefully acknowledged. F.L.M. acknowledges financial support from CNPq.

APPENDIX: RECURSION RELATIONS

We present next an outline of the derivation of the recursion relations for all C_n's. It is based on an extension of the usual procedure [15,16] adapted to our specific synaptic matrix. The main step is the recursion relation for the correlation between any two microscopic overlaps with the noncondensed patterns that enter in Eq. (9).

We start with the definition of the average

$$\overline{\langle M_N'^{\mu} M_N'^{\nu} \rangle} = \frac{1}{N^2} \sum_{ij} \overline{\xi_i'^{\mu} \xi_j'^{\nu} \langle S_i' S_j' \rangle} \tag{A1}$$

for μ, $\nu = c+1, \ldots, p$, in which the primed (unprimed) variables refer to layer $l+1$ (l), respectively. The averages are explicitly calculated only with respect to primed variables since the averages over the underlying unprimed variables in the lower layer are taken care of by means of the law of large numbers. Writing Eq. (A1) in the form

$$\overline{\langle M_N'^{\mu} M_N'^{\nu} \rangle} = \frac{1}{N^2} \sum_{i} \overline{\xi_i'^{\mu} \xi_i'^{\nu}} + \frac{1}{N^2} \sum_{i \neq j} \overline{\xi_i'^{\mu} \xi_j'^{\nu} \langle S_i' \rangle \langle S_j' \rangle} \tag{A2}$$

allows us to take the thermal averages, leaving, in our case of binary patterns,

$$\overline{\langle M_N'^{\mu} M_N'^{\nu} \rangle} = \frac{\delta_{\mu\nu}}{N} + \frac{1}{N^2} \sum_{i \neq j} \overline{\tanh(\beta \xi_i'^{\mu} h_i') \tanh(\beta \xi_j'^{\nu} h_j')}, \tag{A3}$$

using the fact that the patterns are uncorrelated variables with $\overline{\xi_i'^{\mu} \xi_i'^{\nu}} = \delta_{\mu\nu}$. The embedding field $\xi_i'^{\mu} h_i'$ is given by

$$\xi_i'^{\mu} h_i' = \xi_i'^{\mu} (\boldsymbol{\xi}' \cdot \boldsymbol{A}\boldsymbol{m}) + Q_N^{\mu} + \xi_i'^{\mu} \omega_i', \tag{A4}$$

where $\{\omega_i'\}$ is a set of independent Gaussian random variables $\omega_i' = \sum_{\rho \neq \mu}^{p} \xi_i'^{\rho} Q^{\rho}$ with mean $\overline{\omega_i'} = 0$ and width Δ defined by Eq. (6). Incidentally, the same expression for the embedding field without the need of separating a single term on the right may be used to obtain the recursion relation for the overlap components that yield Eq. (8).

Turning now to the configurational average in Eq. (A3) over primed variables, it decouples into a product of averages. Making an expansion to leading order in $Q_N^{\mu} = O(1/\sqrt{N})$ we obtain

$$\overline{\tanh(\beta\xi_i'^{\mu}h_i')} = \overline{\tanh\,\beta[\xi_i'^{\mu}(\boldsymbol{\xi}'\cdot\boldsymbol{Am}) + \xi_i'^{\mu}z_i']} + \beta Q_N^{\mu}\{\overline{1-\tanh^2\,\beta[\xi_i'^{\mu}(\boldsymbol{\xi}'\cdot\boldsymbol{Am}) + \xi_i'^{\mu}z_i']}\}. \tag{A5}$$

Averaging first with respect to the variable $\xi_i'^{\mu}$ and then taking the configurational average over the Gaussian variable, we obtain

$$\overline{\tanh(\beta\xi_i'^{\mu}h_i')} = KQ_N^{\mu}, \tag{A6}$$

in which $K=\beta(1-q)$, with q defined in Eq. (10). Substituting Eq. (A6) in (A3) we obtain, to $O(1/N)$,

$$\overline{\langle M_N'^{\mu}M_N'^{\nu}\rangle} = \frac{\delta_{\mu\nu}}{N} + K^2Q_N^{\mu}Q_N^{\nu}. \tag{A7}$$

We can now apply Eq. (9) to layer $l+1$ and write it in terms of the correlations $\overline{\langle M_N'^{\mu}M_N'^{\nu}\rangle}$ with the aid of Eq. (7). Then, Eq. (A7) yields the $p-c$ recursion relations

$$\Delta'^2 = b^2(\alpha + K^2\Delta^2) + 4b(1-b)K^2C_1^2 + 2(1-b)^2K^2(\alpha/K^2 + \Delta^2 + C_2^2), \tag{A8}$$

$$C_1'^2 = b^2K^2C_1^2 + 2b(1-b)K^2(\alpha/K^2 + \Delta^2 + C_2^2) + (1-b)^2K^2(3C_1^2 + C_3^2), \tag{A9}$$

$$C_2'^2 = b^2K^2C_2^2 + 2b(1-b)K^2(C_1^2 + C_3^2) + (1-b)^2K^2(\alpha/K^2 + \Delta^2 + 2C_2^2 + C_4^2), \tag{A10}$$

up to

$$C_n'^2 = b^2K^2C_n^2 + 2b(1-b)K^2(C_{n-1}^2 + C_{n+1}^2) + (1-b)^2K^2(C_{n-2}^2 + 2C_n^2 + C_{n+2}^2), \tag{A11}$$

in which $n=3,4,\ldots,p-c-1$, and these equations have to be solved numerically.

The extension to Q-state neurons and patterns, for $Q\geqslant 3$ is straightforward, as well as for continuous neurons.

[1] L. F. Cugliandolo and M. V. Tsodyks, J. Phys. A **27**, 741 (1994).
[2] A. C. C. Coolen, in *Handbook of Biological Physics IV: Neuro-Informatics and Neural Modeling*, edited by F. Moss and S. Gielen (Elsevier, Amsterdam, 2001), p. 619.
[3] A. Düring, A. C. C. Coolen, and D. Sherrington, J. Phys. A **31**, 8607 (1998).
[4] K. Kitano and T. Aoyagi, J. Phys. A **31**, L613 (1998).
[5] M. Kawamura and M. Okada, J. Phys. A **35**, 253 (2002).
[6] W. K. Theumann, Physica A **328**, 1 (2003).
[7] K. Mimura, M. Kawamura, and M. Okada, J. Phys. A **37**, 6437 (2004).
[8] T. Uezu, A. Hirano, and M. Okada, J. Phys. Soc. Jpn. **73**, 867 (2004).
[9] Y. Miyashita and H. S. Chang, Nature (London) **331**, 68 (1988).
[10] Y. Miyashita, Nature (London) **335**, 817 (1988).
[11] M. Griniasty, M. V. Tsodyks, and D. J. Amit, Neural Comput. **5**, 1 (1993).
[12] N. Brunel, Network Comput. Neural Syst. **5**, 449 (1994).
[13] See G. Mongillo, D. J. Amit, and N. Brunel, Eur. J. Neurosci. **18**, 2011 (2003), for a recent review.
[14] A. C. C. Coolen and D. Sherrington, J. Phys. A **25**, 5493 (1992).
[15] F. L. Metz and W. K. Theumann, Phys. Rev. E **72**, 021908 (2005).
[16] E. Domany, W. Kinzel, and R. Meir, J. Phys. A **22**, 2081 (1989); R. Meir and E. Domany, Phys. Rev. Lett. **59**, 359 (1987).
[17] F. L. Metz and W. K. Theumann (unpublished).
[18] *The Handbook of Brain Theory and Neural Networks*, edited by M. A. Arbib (MIT Press, Cambridge, MA, 1995).